



## PROGRESS AND OUTLOOK ON FEW COMPONENT COMPOSITE SOLID STATE ELECTROLYTES

Chavis A. Stackhouse,<sup>1</sup> Alyson Abraham,<sup>1</sup> Kenneth J. Takeuchi,<sup>1,2</sup> Esther S. Takeuchi,<sup>1,2,3</sup>  
Amy C. Marschilok<sup>1,2,3,\*</sup>

<sup>1</sup>Department of Chemistry, Stony Brook University, Stony Brook, NY 11794

<sup>2</sup>Department of Materials Science and Chemical Engineering, Stony Brook University, Stony Brook, NY 11794

<sup>3</sup>Energy and Photon Sciences Directorate, Brookhaven National Laboratory, Upton NY 11973

\*Corresponding author: amy.marschilok@stonybrook.edu

### ABSTRACT

*Lithium solid-state composite electrolytes (LiSCEs) provide the opportunity for long life spans, low self-discharge, high reliability, high energy density, and safety. Additionally, this class of electrolytes can be used in electrolytically formed solid-state batteries (EFBs), which may promote reductions in cell manufacturing costs due to their simplicity of design and permit the formation of batteries with diverse architectures. Herein, we provide a discussion of LiSCEs, highlight some of the recent progress in EFB development, and present a forward outlook.*

### INTRODUCTION:

The advancement and growth of civilization comes with demands in power consumption which present challenges in energy storage, conversion and distribution. The lithium ion battery (LIB) has been an attractive candidate to assuage global energy concerns for various energy applications. The LIB system offers numerous advantages, including long life spans, little self-discharge, high degree of reliability, high energy

density, minimal memory effects, and a range of operating temperatures [1]. LIBs and derivative systems are being actively investigated as solutions for energy applications in electric and hybrid electric vehicles, portable electronics, and wearables devices, such as flexible displays, and microelectromechanical systems (MEMs) [1,2]. However, traditional LIBs have limitations including safety issues associated with lithium dendritic formation and flammable, reactive organic electrolytes [3]. In addition to safety considerations, new manufacturing processes will need to be developed to accommodate a wider variety of operating environments and form factors as the demand for advanced energy storage devices increases.

In the pursuit of malleable, reliable and safer electrolyte systems, solid electrolytes represent an intriguing alternative owing to a reportedly higher thermal stability, absence of liquid electrolyte, larger electromechanical stability window, potential resistance to shock and vibration and, dependent upon electrolyte additives, a tuneable elastic modulus allowing for a higher degree of processability and flexibility. Amongst different solid electrolyte systems; which include garnet solid-state electrolytes [1], sodium super ionic conductor (NASICON) electrolytes, and lithium phosphorus oxy-nitride (LiPON) electrolytes; polymer electrolytes exhibit the greatest degree of tractability and interfacial compatibility, while maintaining the safety characteristics of a solid state electrolyte [4]. Notably, lithium/iodine (Li/I<sub>2</sub>) cells forming a lithium iodide electrolyte are widely employed in implantable cardiac pacemakers [5,6]. Lithium solid-state composite electrolytes (LiSCEs), a variant of solid polymer electrolytes defined by “the combination of nanoparticles and solid-state addition compounds based on the reactions of lithium iodide and small organic molecules” [7] preserve many of the propitious characteristics of solid-state polymer electrolyte. In addition, LiSCEs display advancements in the form of high ionic conductivity. Furthermore, novel LiSCEs have facilitated the investigation of electrolytically formed solid-state batteries (EFBs) [8,9] which allow for an unique approach to reducing cell manufacture costs while simultaneously permitting the formation of batteries with demanding architectures. Herein, we provide a discussion of LiSCEs, highlight some of the recent progress in EFB development, and present some forward outlooks.

## LITHIUM SOLID-STATE COMPOSITE ELECTROLYTES

The use of additives to increase the conductivity, as well as augment other facets of the LIB system has been well established as evinced by earlier work [10]. It was demonstrated that the introduction of calcium iodide to lithium iodide crystals to form a solid solution induced Schottky defects which in turn produced greater ionic conductivity. In pursuit of fast lithium ion conductors [11], a series of lithium halide compounds were investigated; the highest performing of which, LiI·4CH<sub>3</sub>OH, exhibited an ionic conductivity at room temperature of  $2.7 \times 10^{-3} \Omega^{-1}\text{cm}^{-1}$  with an activation enthalpy of 0.36 eV. Single-crystal X-ray diffraction revealed the crystal structure wherein lithium ions are coordinated in a tetrahedral geometry to the oxygen atoms of the methanol molecules, producing  $[\text{Li}(\text{CH}_3\text{OH})_4]^+$  units. The hydroxyl moiety of the methanol acts as a hydrogen bond donor with the iodide anion. Alternately filled and unfilled tetrahedral vacancies compressed within the iodine matrix provide a preferential path for ion conductance within the crystal.

Following the above work, 3-hydroxypropionitrile (HPN) was used as an organic additive to produce a novel lithium composite electrolyte by incorporating both a hydroxyl and a cyano group as coordination capable moieties showing intriguing properties. [12,13] The obtained compound exhibited ionic conductivity reliant upon the LiI content present, shown in Figure 1a, with a maximum of  $6.97 \times 10^{-3} \text{ S/cm}$  when

LiI/HPN = 1:15. LiI/HPN<sub>x</sub> shows an extreme decrease conductivity from  $3.1 \times 10^{-3}$  S/cm to  $2.36 \times 10^{-6}$  S/cm as the molar ratio of LiI to HPN increases from 1:4 to 1:2; however, a further increase in salt content produce greater conductivity up to a second maximum of  $1.1 \times 10^{-4}$  S/cm as the ratio approaches 2:1. This dependence shown above 1:2 is irregular in comparison to contemporary electrolytes, yet congruent with the behaviour displayed by polymer-in-salt electrolytes. Mass spectrometry analyses at various LiI/HPN ratios detected an abundance of small molecules, e.g. Li(HPN)<sub>2</sub> and CH<sub>2</sub>CH<sub>2</sub>CN—Li—OCH<sub>2</sub>CH<sub>2</sub>CN, thus implying exclusive employment of small molecule does not preclude polymer-in-salt behaviour [13]. Investigations via FTIR indicate the disappearance of the strong peak at  $3417 \text{ cm}^{-1}$  and a concurrent appearance at  $3217 \text{ cm}^{-1}$ , see Figure 1b, to suggest the dissociation of hydrogen bonding in the pure organic additive as the lithium cation associates with the hydroxyl group. This behaviour aligns with the LiI/HPN ratio ranges for normal conduction. Addition of excess LiI produces a broad peak at  $3489 \text{ cm}^{-1}$  due to hydrogen bonding between the iodide anion and the hydroxyl moiety of HPN; the band's intensity eclipses the  $3217 \text{ cm}^{-1}$  band at LiI/HPN = 2:1. The intensity of the  $3489 \text{ cm}^{-1}$  band demonstrates the preference of the hydrogen bonding between the iodide and the hydroxyl group over the interaction of the hydroxyl with the lithium cation. The priority of the hydrogen bonding guarantees continuous network and behaviour as a solid electrolyte [13-15].

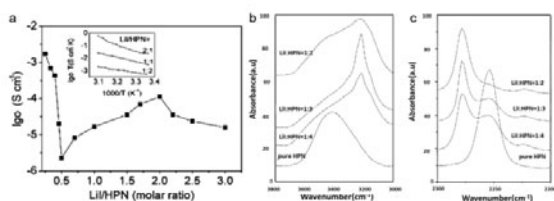


Figure 1: (a) The salt content dependence of conductivity of LiI/HPN electrolyte at 30 °C (inset: Arrhenius plots of conductivity of the composites at different molar ratios of LiI/HPN). FTIR spectra of (b) the OH stretching, (c) the CN stretching. Figure 1a is reprinted with permission from Ref. 13. Copyright 2004 Royal Society of Chemistry. Figures 1b,c are reprinted with permission from Ref. 12 Copyright 2004, The Electrochemical Society.

Unlike reported observations of the hydroxyl moiety, the nitrile band that appears at  $2254 \text{ cm}^{-1}$  displays a hypsochromic shift to  $2277 \text{ cm}^{-1}$  to demonstrate increasing *s* character of the nitrile bond resultant of the association the nitrile group with the lithium cation, shown in Figure 1c. The trend continues in correlation to increasing LiI content until the  $2254 \text{ cm}^{-1}$  band become nearly imperceptible at the LiI/HPN ratio of 1:2, indicating the near uniform coordination of the nitrile moiety to the lithium cation. The association of the nitrile group displays preference over that of the hydroxyl at low LiI loadings, up to 1:40 LiI/HPN, after which hydroxyl association may be observed [12-14]. The associations to the lithium cation limit its mobility and allow for a high transference number of the iodide anion. Upon increasing the salt content, the  $2277 \text{ cm}^{-1}$  bands display some broadening accompanied by a new component at  $2280 \text{ cm}^{-1}$  that becomes further differentiated with greater salt concentration. The behaviour of the  $2280 \text{ cm}^{-1}$  peak is analogous to spectroscopic observations of polyacrylonitrile electrolytes that feature a polymer-in-salt conduction behaviour. This band is related to the interaction of the nitrile moiety with  $\text{Li}_m^+ \text{I}_n^-$  ( $m > n$ ) ionic clusters within the LiI/HPN composite electrolyte. The nitrile group may form regular  $\text{Li}^+ \cdots \text{CN}$  aggregates when interacting

with singular lithium cations and, alternatively, the ionic clusters can produce aggregates with the nitrile within the HPN molecule. However, the nitrile group displays a preference for the ionic clusters over that the singular lithium cations due the clusters' stronger polarity in comparison. Further increasing of salt content imparts greater ionic cluster content. As such, increasing salt content results in the decreasing of the relative intensity  $2277\text{ cm}^{-1}$  band with an increase in that of the  $2280\text{ cm}^{-1}$  band. The new band heralds the transition in the composite electrolyte conductivity at higher salt contents. The ionic clusters support the LiI/HPN electrolyte polymer-in-salt conduction property. At lower salt loadings, the ionic clusters form percolation pathways segments that facilitate charge exchanges with ionic species associated with the HPN molecule. The cooperation of the percolation pathway segments with the aforementioned ionic species perform as a transient bridge through which charge exchange may occur and as a result the polymer-in-salt property becomes apparent. Increasing the salt loading allows for the respective cluster segments to interconnect and produce percolation pathways through development of both short and long ionic chains. This creates a bridge of greater permanence as a powerful vehicle for ion transport within the electrolyte [13,14].

A series of electrolytes obtained by means of the combination of succinonitrile, lithium iodide, and iodine (SN-LiI-I<sub>2</sub>) represents another recent LiSCE of note. The SN-LiI-I<sub>2</sub> electrolyte takes advantage of the plastic crystalline nature of succinonitrile, which features trans-gauche isomerization [16,17]. Trans isomers may behave as impurities to produce vacancies within the crystal lattice and impart high molecular diffusivity. As such, the structure lends itself to ion transport in the plastic phase environment to result in a high electrical conductivity. While maintaining the iodine to lithium iodide ratio at 10%, increasing the LiI to succinonitrile ratio from 0 to 5% showed a marked increase in conductivity to a high of  $\sim 1.6 \times 10^{-3}\text{ S/cm}$  at 25°C. Further increase past 5% produces inhomogeneity in the obtained electrolyte. The conductivity shows an exponential rise as the ratio approaches 5% and simultaneously the electrolyte relative conductivity enhancement shows an exponential decrease. This behaviour has been attributed to free ion generation and interaction phenomena as the salt content increases.

## SELF-FORMING OR ELECTROLYTICALLY FORMED BATTERIES

Growing interest to improve battery technology, with respect to minimizing manufacturing costs and facilitating conformal adaptation to a wider array of operating

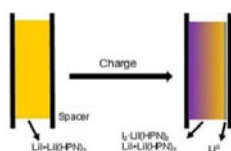


Figure 2: LiI battery: As assembled (left), and after charge (right) with Li metal anode and I<sub>2</sub>-based cathode. Reproduced with permission from Ref. 20. Copyright 2018, The Electrochemical Society.

environments and form factors, has led to the introduction of self-forming or electrolytically-formed batteries wherein the anode and cathode is formed in situ on the atomic level from a homogeneous composite material upon the application of a voltage [8,9,18,19,20]. At sufficient voltage for oxidation of the composite, lithium metal forms at the anode as a result of a reduction process; the corresponding oxidation process induces the formation of a polyiodide species at the positive electrode, as depicted in

Figure 2. LiSCEs lend well to this approach of self-assembly and represent prime candidates for the further development of this technology. AC impedance studies of a battery constructed using a composite constructed from hydrated lithium iodide and poly(vinyl-pyrrolidone) (PVP) depicted an AC impedance response of an ionic conductor in the pre-formed stage [9]. In situ measurement of the EFB afforded the development of three depressed semicircles in the impedance spectrum to confirm the transformation of the precursor electrolyte to anodic and cathodic regions. Nyquist plots from low to high  $\text{Re}(Z)$  and from high to low frequency declared the depressed semicircles to correspond to ionic conduction of the electrolyte, ionic conduction of the solid electrolyte interface, and charge transfer processes within the cathode.

The feasibility of this approach was demonstrated [20] employing an LiSCE,  $\text{LiI}(\text{HPN})_2$ , in the construction of an electrolytically generated rechargeable  $\text{LiI}/\text{I}_2$  cell (Figure 3). Conductivity measurements of a solid electrolyte with 80Li-20  $\text{Li}(\text{HPN})_2$  (by mass) composition showed a conductivity of  $1.7 \times 10^{-7} \text{ S/cm}$ , and was used for subsequent electrochemical testing. The transition of the solid electrolyte from the precursory composite to differentiated anode and cathode was confirmed using x-ray

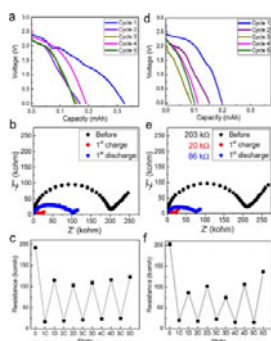


Figure 3: a,d) Discharge capacities cycles 1–5, b,e) AC impedance before charge, after the 1st charge step, and after the 1st discharge step, c,f) Fitted resistance at the end of discharge and charge steps for cells charged to a-c) 5% and (d-f) 10% state of charge. Reproduced with permission from Ref. 20. Copyright 2018, The Electrochemical Society.

diffraction before and after charge. The appearance of peaks at 2-theta values of  $8.6^\circ$ ,  $16.9^\circ$ ,  $25.3^\circ$ ,  $33.8^\circ$ ,  $42.4^\circ$ , and  $51.4^\circ$ , each of which respectively correspond to the (001), (002), (003), (004), (005), and (006) diffraction planes of  $\text{I}_2\text{-LiI}(\text{HPN})_2$  [21] indicating iodine formation at the positive electrode. An OCV of  $\sim 2.7\text{V}$  verified the presence of the  $\text{Li}/\text{I}_2$  couple. Prior to charging, the cells displayed resistance values of 200-300 k $\Omega$ . Initial charging promoted a distinct decrease in impedance, see Figure 3b,e. A five-fold decrease in resistance was observed upon obtaining 5% of the theoretical charge capacity and the resistance remained reduced, at  $\sim 30\text{-}40 \text{ k}\Omega$ , with some minor variation with additional charging. The authors attribute the source of the reduction to decreased interfacial resistance upon the formation of the lithium anode and iodine cathode. Galvanostatic cycling to probe the feasibility as a secondary cell elicited discharge capacities  $>0.1 \text{ mA h/g}$  that were over five cycles, suggesting reversibility, Figure 3a,d. The reduced impedance also remained consistent over the five cycles, displaying a lower impedance of  $\sim 20 \text{ k}\Omega$  at the end of each charge step and a higher impedance at end of each corresponding discharge step for cells charged to 5% and 10% charge, as shown in Figure 3c, f, respectively.

## FUTURE OUTLOOK

Lithium solid-state composite electrolytes can impart many desirable characteristics into batteries such as long life spans, low self-discharge, high degree of reliability, high energy density, and safety. The promise of electrolytically formed solid-state batteries includes the favourable characteristics noted above and also the opportunity for reductions in cell manufacturing costs and permitting the formation of batteries with demanding architectures. Full realization of the potential of these materials shall hinge upon demonstration of extended cyclability and performance within ambitious device designs.

## ACKNOWLEDGMENTS

This work was supported by the U. S. Department of Energy Office of Energy Efficiency and Renewable Energy under the Advanced Battery Materials Research program, award DE-EE0007785. C.S. acknowledges support from the NIH Institutional Research and Academic Career Development Award and New York Consortium for the Advancement of Postdoctoral Scholars (IRACDA-NYCAPS), award K12-GM102778. A.A. acknowledges the Graduate Assistance in Areas of National Need Fellowship (GAANN). E.S.T. acknowledges the William and Jane Knapp Chair in Energy and the Environment.

## REFERENCES

- [1] S. Teng, J. Tan, A. Tiwari, *Curr. Opin. Solid State Mater Sci*, **18**(1), 29 (2014).
- [2] P. Hu, J. Chai, Y. Duan, Z. Liu, G. Cui, and L. Chen, *J. Mater. Chem. A.*, **4**(26), 10070 (2016).
- [3] Z. Zhang, Y. Shao, B. Lotsch, Y.-S. Hu, H. Li, J. Janek, L. F. Nazar, C.-W. Nan, J. Maier, M. Armand, L. Chen, *Energy Environ. Sci.*, **11**(8), 1945 (2018).
- [4] N. J. Dudney, W. C. West, J. Nanda, Eds. *Handbook of Solid State Batteries*, 2<sup>nd</sup> ed. (Singapore: World Scientific Publishing Co., 2015).
- [5] D. C. Bock, A. C. Marschilok, K. J. Takeuchi, and E. S. Takeuchi, *Electrochim. Acta*, **85**, 155 (2012).
- [6] E. S. Takeuchi and R. A. Leising, *MRS Bull.*, **27**(8), 624 (2002).
- [7] D. Li, D. Qin, M. Deng, Y. Luo, Q. Meng, *Energy Environ. Sci.*, **2**(3), 283 (2009).
- [8] W. Yourey, L. Weinstein, A. Halajko and G. G. Amatucci, *Electrochim. Acta*, **66**, 193 (2012).
- [9] L. Weinstein, W. Yourey, J. Gural and G. G. Amatucci, *J. Electrochem. Soc.*, **155**(8), A590 (2008).
- [10] C. R. Schlaikjer and C. C. Liang, *J. Electrochem. Soc.*, **118**(9), 1447 (1971).
- [11] W. Weppner, W. Welzel, R. Kniep and A. Rabenau, *Angew. Chem. Int. Ed.*, **25**(12), 1087 (1986).
- [12] H. X. Wang, B. F. Xue, Y. S. Hu, Z. X. Wang, Q. B. Meng, X. J. Huang, L. Q. Chen, *Electrochem. Solid-State Lett.*, **7**(10), A302 (2004).
- [13] H. Wang, Z. Wang, B. Xue, Q. Meng, X. Huang, L. Chen, *Chem. Commun.*, **19**, 2186, (2004).
- [14] H. X. Wang, Z. X. Wang, H. Li, Q. B. Meng, L. Q. Chen., *Electrochim. Acta*, **52**(5), 2039 (2007).
- [15] F.-C. Liu, W.-M. Liu, M.-H. Zhan, Z.-W. Fu and H. Li. *Energy Environ. Sci.*, **4**(4), 1261 (2011).
- [16] R. K. Gupta, I. Bedja, A. Islam, and H. Shaikh, *Solid State Ionics*, **326**, 166 (2018).
- [17] R. K. Gupta and H.-W. Rhee, *Electrochim. Acta*, **76**, 159 (2012).
- [18] W. Yourey, L. Weinstein, and G. G. Amatucci, *Solid State Ionics*, **204**, 80, (2011).
- [19] W. Yourey, L. Weinstein, A. Halajko, and G. G. Amatucci, *ECS Trans.*, **28**(30), 159, (2010).
- [20] A. Abraham, J. Huang, P. F. Smith, A. C. Marschilok, K. J. Takeuchi, and E. S. Takeuchi, *J. Electrochem. Soc.*, **165**(10), A2115 (2018).
- [21] F.-C. Liu, Z. Shadikie, F. Ding, L. Sang, and Z.-W. Fu, *J. Power Sources*, **274**, 280, (2015).